Ideal Topographic Simulations for Null Measurement Data

Yan-Jen Su[1,#], Chi-Hong Tung[1], Leh-Rong Chang[1], Jin-Liang Chen[1] and Calvin Chang[1]

1 Instrument and Sensor Development Division, Center for Measurement Standards, Industrial Technology Research Institute, Hsinchu, Taiwan
Corresponding Author / E-mail: YJSu@itri.org.tw, TEL: +886-3-573-2160, FAX: +826-3-572-2383

KEYWORDS : Hole filling, Reconstruction, Modeling

A method is described for ideally reconstructing the profile from a surface profiling measurement containing a reasonable amount of null measurement data. The proposed method can conjecture lost information and rectify irregular data that result due to bad measuring environments, signal transmission noise, or instrument-induced errors. The method adopts the concept of computer graphics and consists of several processing steps. First, a search for valid data in the neighborhood of the null data is performed. The valid data are then grouped and their contours are extracted. By analyzing these contours, a bounding box can be obtained and the general distribution of the entire area encompassing the valid and null data is determined. Finally, an ideal surface model is overlaid onto the measurement results based on the bounding box, generating a complete reconstruction of the calculations. A surface-profiling task on a liquid crystal display photo spacer is used to verify the proposed method. The results are compared to those obtained through the use of a scanning electron microscope to demonstrate the accuracy of the proposed method.

Manuscript received: October 2, 2007 / Accepted: July 2, 2008

1. Introduction

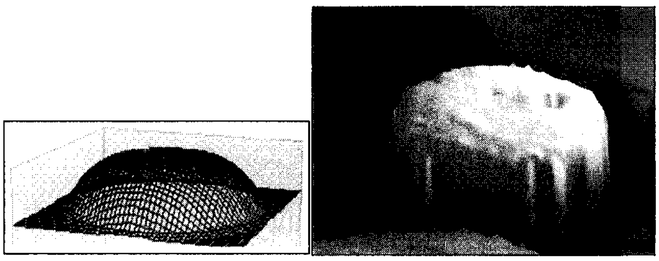

(a) (b)

Fig. 1 (a) Actual topography of the hill-shaped LCD spacer as measured by the SEM (b) White light interferometer results The edge area could not be detected by the reflected light, producing null measurement data

Light interferometric technology allows for fast, extremely fine, nondestructive inspections, and is therefore widely used for micro-substance measurements. Surface topographies with high inclinations, however, cannot be correctly detected due to the wide angle of the reflected light, resulting in insufficient measurement data. Figure 1 shows that the actual topography of a liquid crystal display (LCD) spacer, as measured using a scanning electron microscope (SEM), should be shaped like a hill. But because the edge area inclination is too high (>20°), the light interferometer results indicate null measurement data around the edges.

This problem is commonly handled by using numerical methods[1] to fit the measured input data. The null fields are then reconstructed using the fitted curves or surfaces. The least squares method is a common approach; by estimating the degree of the result, it can produce an approximate curve that has a minimal square difference with the input data. Splines are widely applied as well since they produce smooth results that are closer to the input data by consolidating continuous basis functions.

The most obvious disadvantage of the least squares method is that the expressed topography of a polynomial is limited and not suitable for all possible situations. Splines, however, are easily affected by noise and create oscillation problems. A low-pass filter can be applied to reduce the noise before fitting, but this alters the originally measured results.

To overcome the problems encountered when using traditional numerical methods, we propose an algorithm that can reconstruct the lost data from high-inclination topographies based on the limited measuring information and optical limits. We describe the reconstruction accuracy, process speed, and stability of our model, and consider the noise and robustness of the resulting surface topography.

2. Related Work

2.1 Simulation

Carr et al[2] authored a widely quoted thesis on data reconstruction. They used radial basis functions to calculate space enantiomeric implicit functions that can be both accurate and smooth simultaneously, and they used an implicit function to reconstruct the data. While calculating the implicit functions, they reduced the number of calculations required to determine the radial basis function, increasing the calculation speed to obtain a large quantity of data

(>300,000 data points) in under 3 min. Their method included a data parameter that could be used to adjust the smoothness, giving the user complete control over the implicit function. The method used the marching cubes technique[3,4] to reconstruct the curved iso-surface from the implicit functions. And Yoo[5] applied domain decomposition method to reduce the complication of computing.

Davis et al.[6] used diffusion to extend the Curless and Levoy[7] distance function concept of the topography pending reconstruction. They then applied marching cubes to the distance function to obtain an iso-surface, and used this in an iterative fashion until the surface contour was completely reconstructed. Their method only requires data points around the pending topography to reconstruct and calculate the iso-surface. The storage space is much smaller than that required by Carr et al.,[2] and the calculations are much simpler.

Nooruddin and Turk[8] took a 2D imagery method and extended it to 3D data. First, they changed the surface contours into voxels to eliminate the thin-shelled situation. They then used accelerated imaging of the distance function to process the Gonzalez and Woods[9] closing calculation method to patch null data. Finally, they used marching cubes to reconstruct the iso-surface. This method of calculation is simple and the data obtained after reconstruction are smooth, but all of the data points are required during the calculations.

Pauly et al,[10] compared the pending contour to all models stored in a database, and then picked the closest one. By applying the least error principle to complete the reconstruction, they adjusted the infrastructure of the model and then laid it on top of the pending contour. They then returned the results to the database to expand its contents. The great advantage of this method over the others is that the null data pending reconstruction can have a great range. The problem encountered in real-life applications is how to effectively adjust the known model.

3. Applied Method

In the present study, we adapt the method of Pauly et al.[10] to obtain more accurate reconstruction results and provide a more convenient method of applying the model. We describe an effective registration approach and interpolation means to reconstruct the spacer shown in Fig. 1.

3.1 Constructing the model

Because the spacer is axisymmetrical, we used the following steps to reconstruct the spacer model, as illustrated in Fig. 2.

1. Obtain the side contour using a SEM to measure the spacer.
2. Use half of the side contour and rotate around an imaginary symmetrical axis once. This type of revolution is a common method of constructing a model in computer-aided geometric design.[11]
3. The result of the side contour rotation gives a model for the spacer. This model is the bounding box whose parameter space is in the interval of [0,1], and is used with and laid on the pending topography in world space.

3.2 Bounding box search for the pending topography

After constructing the parameter space, we require the pending topography in world space for overlaying purposes. The steps, illustrated in Fig. 3, are as follows.

1. Use a threshold to obtain the pending spacer since the spacer holds the panels and has a greater height.
2. Obtain the complete contour data points of the spacer using chain rule searching,[9] a common image handling method that repeatedly searches for neighboring contour points by using four-neighborhood or eight-neighborhood techniques.
3. Apply a multiplier to the contour data points. The value with the least error gives the most suitable equation for spreading the data along the long axis of the bounding box. When the largest error equation is used for the short axis of the bounding box, the two axes have a positive relationship. The tightest-fitting bounding box is formed by adding the maximum height of the spacer and the base height.

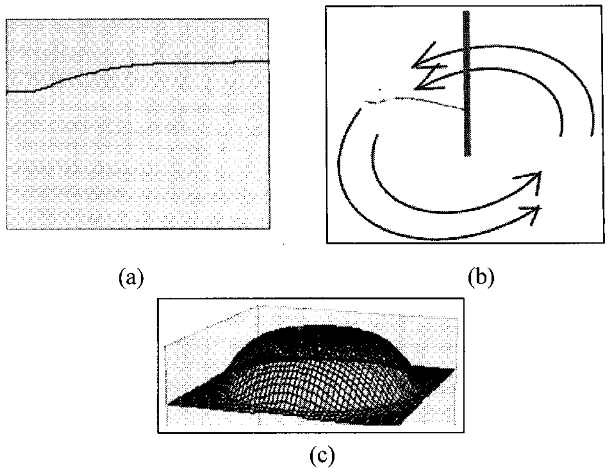

Fig. 2 Spacer reconstruction method (a) obtain the side profile of the spacer contour from SEM measurements (b) rotate once about the side contour (c) the surface contour after rotation becomes the model in [0,1] bounding box parameter space

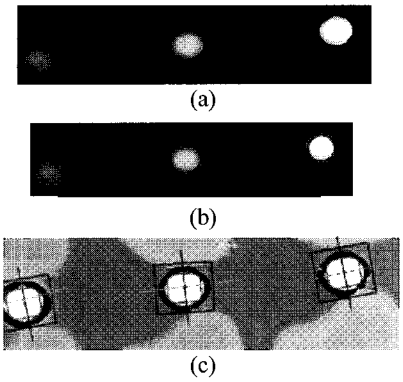

Fig. 3 Search method for the bounding box of the pending topography (a) use a threshold to obtain the pending spacer (b) find the contour data point of the spacer using chain rule searching and (c) use the least squares method based on the bounding data points to find the tightest-fitting bounding box

3.3 Bounding box search for the pending topography

The bounding box in parameter space is overlaid onto the bounding box of the pending topography in world space, completing the reconstruction of the spacer, as illustrated in Fig. 4(a). However, an aliasing problem occurs since the original measured data and the reconstructed model are not continuous, as shown in Fig. 4(b). Therefore, we include smoothness calculations in the overlay, which induce a better match between the model and measured data.

The model can be further adjusted according to the measured data after it is mapped into object space. The model sampling height inside the bounding box is stretched to match the measured data and obtain a scale ratio. All samples of the model are then assigned a scale ratio by interpolating the known data. Finally, each sample of the model is individually corrected by its scale ratio, as shown by the curve in Fig. 4(c). This method is effective and has a high degree of accuracy.

4. Results

The object used to test the proposed calculation method, shown in Fig. 5(a), is a 640 × 480 LCD panel obtained from a white light interferometer that included three pending reconstruction spacers. The computer system consisted of a 1.8 GHz Intel CPU with 1 GB of RAM running Microsoft Windows XP. The reconstruction is shown in Fig. 5(b). The auto-imaging calculations required 1 s.

Following the testing method of Kobayashi et al[12] figure 6 compares the results obtained before and after the reconstruction with SEM data. We scaled the profiles to the same ratio as the SEM measurements and overlapped them to illustrate any differences. Before reconstruction (Fig. 6(a)), the original data did not include any information about the inclined side, resulting in incorrect contours. After reconstruction (Fig. 6(b)), we obtained a tight curve that matched the profile of the actual object.

We also applied our algorithm to a more complicated bumper that included a multilayer structure and a large inclination. The original data are shown in Fig. 7(a) and the reconstructed results are presented in Fig. 7(b) and (c). Our proposed algorithm recovered the lost information and produced smooth results.

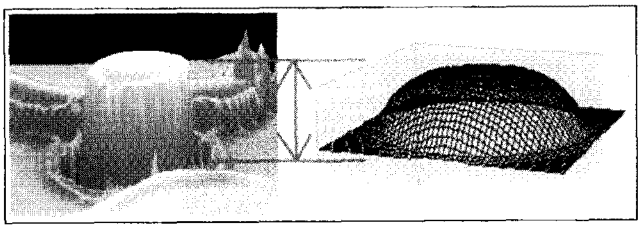

(a)

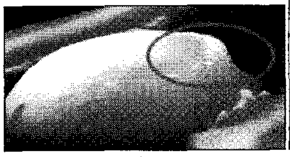

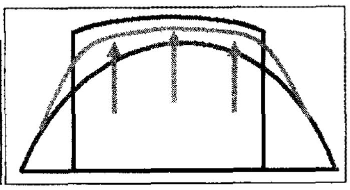

(b) (c)

Fig. 4 (a) Parameter space and bounding box overlay (b) Jagged edge aliasing phenomenon created before smoothing (c) Comparison of known measured data (black line) and the proposed model before smoothing (blue line) and after smoothing, and applying a weighted average (red line)

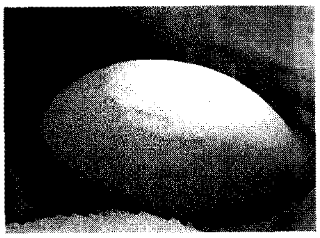

(a) (b)

Fig. 5 (a) Spacer before reconstruction (b) Results after reconstruction

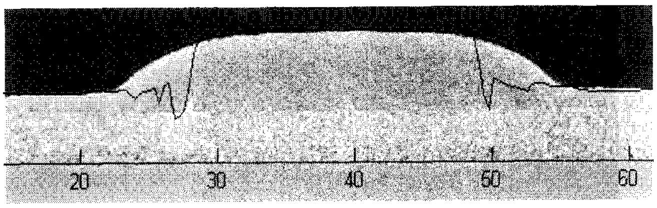

(a)

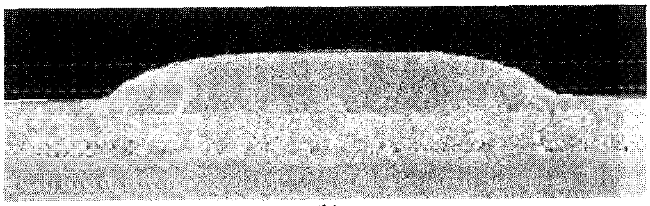

(b)

Fig. 6 (a) Comparison of SEM profiles (gray) and the results obtained from white light interferometry (a) before reconstruction (blue line) and (b) after reconstruction (red line)

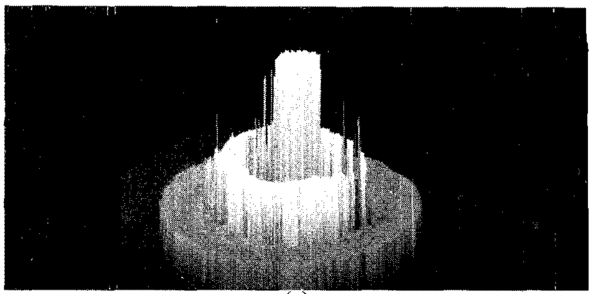

(a)

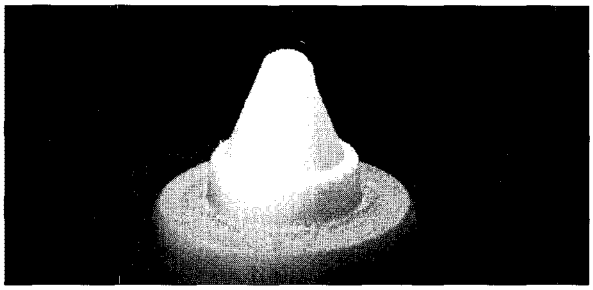

(b)

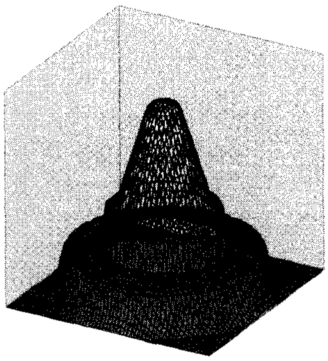

(c)

Fig. 7 (a) Bumper before reconstruction (b) results after reconstruction and (c) the final bumper model

REFERENCES

1. Cheney, W. and Kincaid, D., "Numerical Mathematics and Computing," Brooks Cole, 2004.

2. Carr, J. C., Beatson, R. K., Cherrie, J. B, Mitchell, T. J., Fright, W. R., McCallum, B. C. and Evans, T. R., "Reconstruction and Representation of 3D Objects with Radial Basis Functions," SIGGRAPH, ACM, pp. 67-76, 2001.

3. Lorensen, W. E. and Cline, H. E., "Marching Cubes: A High Resolution 3D Surface Construction Algorithm," SIGGRAPH, ACM, pp. 163-169, 1987.

4. Treece, G. M., Prager, R. W. and Gee, A. H., "Regularised Marching Tetrahedra: Improved Iso-Surface Extraction," Computer and Graphics, Vol. 23, No. 4, pp. 583-598, 1999.

5. Yoo, D. J., "Filling Holes in Large Polygon Models Using an Implicit Surface Scheme and the Domain Decomposition Method," International Journal of Precision Engineering and Manufacturing, Vol. 8, No. 4, pp. 3-10, 2007.

6. Davis, J., Marschner, S. R., Garr, M. and Levoy, M., "Filling Holes in Complex Surfaces Using Volumetric Diffusion," 3DPVT, IEEE, 2002.

7. Curless, B. and Levoy, M., "A Volumetric Method for Building Complex Models from Range Images," Proceedings of the 23rd

annual conference on Computer graphics and interactive techniques, pp. 303-312, 1996.

8. Nooruddin, F. S. and Turk, G., "Simplification and Repair of Polygonal Models Using Volumetric Techniques," Trans. Visualization and Computer Graphics, IEEE, Vol. 9, No. 2, pp. 191-205, 2003.

9. Gonzalez, R. C. and Woods, R. E., "Digital Image Processing," Prentice Hall, 2002.

10. Pauly, M., Mitra, N. J., Giesen, J., Gross, M. and Guibas, L. J., "Example-based 3D Scan Completion," Proceedings of the 3rd Eurographics symposium on Geometry processing, pp. 23-32, 2005.

11. Watt, A., "3D Computer Graphics," Addison-Wesley, 2000.

12. Kobayashi, Y. and Shirai, K., "Multi-axis Milling for Micro-t exturing," International Journal of Precision Engineering and Manufacturing, Vol. 9, No. 1, pp. 34-38, 2008.